EDGES MEMO # 222

MASSACHUSETTS INSTITUTE OF TECHNOLOGY
HAYSTACK OBSERVATORY
WESTFORD, MASSACHUSETTS 01886

December 19, 2016

Telephone: 781-981-5414
Fax: 781-981-0590

To: EDGES Group

From: Alan E.E. Rogers

Subject: Tests of the effect of systematics in the search for absorption signature in low band data.

Features at 84 and 70 MHz were reported in memos 196 and 208. These features were analyzed over 65-95 MHz and 62-80 MHz with 4 terms removed and were initially thought to be due to resonances in the antenna or ground plane but attempts to identify their origin have been unsuccessful and it is now thought that they are most likely part of a broader signature present in the sky noise spectrum. This conclusion has been strengthened by finding that a flattened signature fits the observations with high signal to noise (SNR) ratio. This has been explored and reported in memo #221. In this memo this is explored further with more tests of the effect of instrumental systematics.

Figure 1 shows the result of a search for a signature whose center frequency, width and shape is allowed to vary. The shape is defined by the parameter, τ, discussed in memo 220. It is derived from the signature of an absorption of optical depth τ but does not necessarily mean the signature, if real, has to originate from an absorption of high opacity. Rather it is a convenient way of obtaining a flattened Gaussian with a simple analytic expression. The data in Figure 1 is from 2016_259 to 2016_333. The 4-terms were from the "EDGES" polynomial. The beam correction for the extended ground plane was applied.

Figures 2 through 12 were made with the various changes made listed in Table 1. In each case a range of nighttime data from GHA from 4 to 16 hours is used. Figure 2 shows that using 4 physical terms, (scale, spectral index, spectral index curvature and ionospheric absorption) makes little difference.

Figure 3 shows the best fit Gaussian which clearly doesn't fit as well as the "flattened" signature. Figure 4 shows that a fit over a wider frequency range yields a reasonable fit with close to the same width and center frequency.

Figures 5 through 10 show that the effect of changes in parameters which alter the instrumental bias lower the SNR but still find the best fit signature centered at 78±1 MHz with width of 21±2 MHz and amplitude 0.5±0.2 K.

Fig.	Test	Center MHz	Width MHz	Amplitude K	SNR	rms after fit mK
1	Reference – 4 term polynomial	78	20	0.56	27	31
2	4-term physical function instead of polynomial	78	19	0.46	23	27
3	Fit with Gaussian signature	75	30	2.1	14	48
4	Fit over 55-99 MHz	77	20	0.65	21	51
5	No beam correction	79	23	0.46	12	35
6	No loss correction	77	19	0.46	11	69
7	+100 ps added to antenna S11	77	19	0.67	24	45
8	-100 ps added to antenna S11	78	23	0.50	19	27
9	+0.1 dB added to antenna S11	78	21	0.50	26	26
10	-0.1 dB added to antenna S11	78	20	0.62	20	45
11	Included all nighttime data 2015_284 to 2016_333	78	19	0.64	36	29

Table 1. Best fit signature parameters to test sensitivity to S11 offsets, beam and loss correction and other changes in processing.

Figure 11 shows that including data with the original 10×10 m ground plane also yields a similar signature. Table 2 shows the parameters of the best fit signatures for data over a 6 hours centered at different GHA, except at GHA=16, have the same center frequency, width and amplitude within the errors determined from the fits in Figures 5 through Figure 10.

Figure 12 shows the best fit signature determined using Galaxy calibration also finds a best fit signature with parameters within the same errors. For this test data from 2016_259 to 2016_333 was used with GHA -1.5 to + 1.5 hours for "Galaxy up" and GHA 6.5 to 13.5 hours for "Galaxy down" data. Similar results were obtained for the data discussed in memo 215. While Galaxy calibration help reduce some instrumental errors it is sensitive to beam correction error. All of the "Galaxy up" data currently available with the extended ground plane is during the day and it will be several more months before nighttime data becomes available. The data used to test the Galaxy calibration was filtered to avoid periods of solar activity but may still be effected by the ionosphere.

Some of the quasi-periodic fine structure in the spectra of Figures 1 through 11 is structure in the antenna S11 which was not adequately smoothed the 37 term Fourier series used to smooth the S11. This can be reduced by using a 10 term polynomial. This structure in the antenna S11 is absent in Figure 12 because it is cancelled by the Galaxy Calibration.

GHA hours	Center MHz	Width MHz	Amplitude K	SNR	rms after fit mK
6	79	22	0.68	13	52
8	78	20	0.48	17	40
10	78	19	0.43	18	40
12	78	20	0.53	16	48
14	78	20	0.62	19	60
16	78	20	0.83	13	71

Table 2. Best fit signature parameters for changes in GHA using data from 2016_288 to 2016_298.

All the searches for best fit spectra, except that of Figure 3, were made with the "flattening" parameter, τ=7 because τ is not well determined. The change in best fit signature parameters vs τ are given in Table 3.

τ	center MHz	width MHz	amplitude K	SNR	rms after fit mK
0	75	30	2.1	14	48
1	77	26	1.7	15	45
2	78	23	1.3	19	39
3	78	22	0.89	22	34
5	78	21	0.65	24	31
7	78	20	0.56	25	31
9	78	20	0.51	24	32
20	77	20	0.43	22	34

Table 3 Best fit parameters for reference (Figure 1) vs flattening parameter.

The general trend is for a signature with less flattening signature is to have a lower SNR, a larger amplitude and larger width.

Comments on absorption signature

While the width and redshift of the "flattened" signature are well within the range expected from models (see Pritchard and Loeb 2008 and Fialkov, Barkana and Visbal 2014 for example) the amplitude of the depth of the signature is much larger than those in published models. In this respect even larger depth of the best fit Gaussian, which is not strongly excluded by the data, is even further away from current models. It is noted in memo 221 that a lower kinetic temperature would result in an absorption depth closer to that of the flattened signature amplitude of about 0.5 K. A lower kinetic temperature with recent models of kinetic temperature based on a rapid decline in star-formation rate density (SFRD) at $z > 8$. See Prober et al (2015).

A potential cause of flattening could be that the spin temperature reaches the kinetic temperature and remains constant in the frequency range of 70 to 84 MHz ($19 > z > 16$). This could be assisted by an enhanced coupling of the spin temperature to the kinetic temperature by increased hydrogen density or collisions with molecular hydrogen, deuterated hydrogen or protons (see, Furlanetto and Furlanetto 2007) or more likely stronger Lyman alpha (see Holzbauer et al. 2012) in an environment with higher proton density.

Pober, Jonathan C., Zaki S. Ali, Aaron R. Parsons, Matthew McQuinn, James E. Aguirre, Gianni Bernardi, Richard F. Bradley et al. (2015), PAPER-64 Constraints on reionization. II. The Temperature of the z= 8.4 intergalactic medium." The Astrophysical Journal 809, no. 1: 62.

Oesch, P. A., R. J. Bouwens, G. D. Illingworth, M. Franx, S. M. Ammons, P. G. van Dokkum, M. Trenti, and I. Labbé. (2015), First frontier field constraints on the cosmic star formation rate density at z∼ 10—the impact of lensing shear on completeness of high-redshift galaxy samples. Based on data obtained with the Hubble Space Telescope operated by AURA, Inc. for NASA under contract NAS5-26555. The Astrophysical Journal 808, no. 1: 104.

Loeb, Abraham, Steven R. Furlantetto (2013) The First Galaxies in the Universe, Princeton University Press.

Holzbauer, Lauren N., and Steven R. Furlanetto (2012), Fluctuations in the high-redshift Lyman-Werner and Lyα radiation backgrounds. Monthly notices of the Royal Astronomical Society 419, no.1: 718-731.

Furlanetto, Steven R., and Michael R. Furlanetto. (2007), Spin exchange rates in proton–hydrogen collisions. Monthly Notices of the Royal Astronomical Society 379, no. 1 (2007): 130-134.

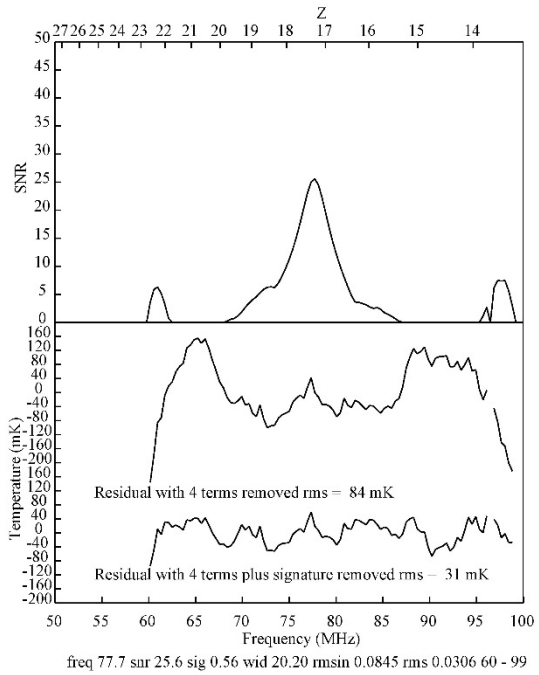

Figure 1.

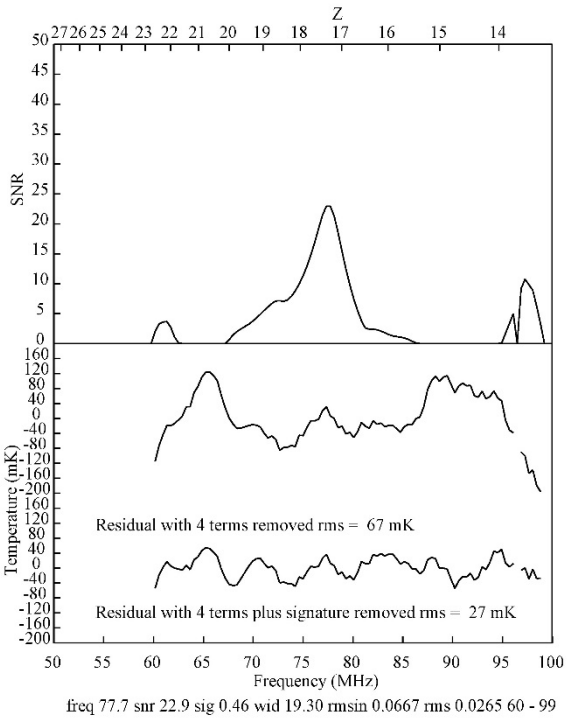

Figure 2.

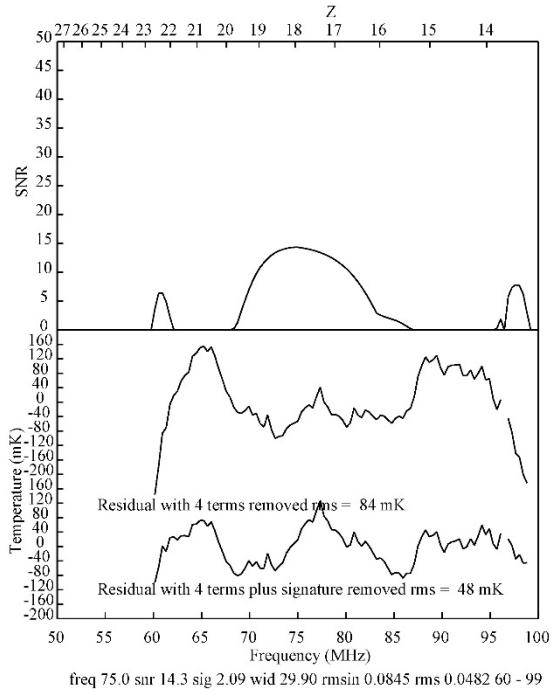

Figure 3.

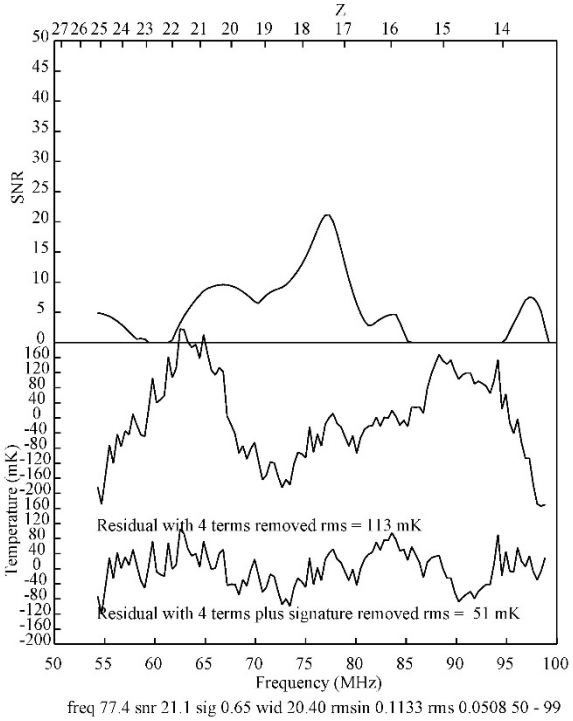

Figure 4.

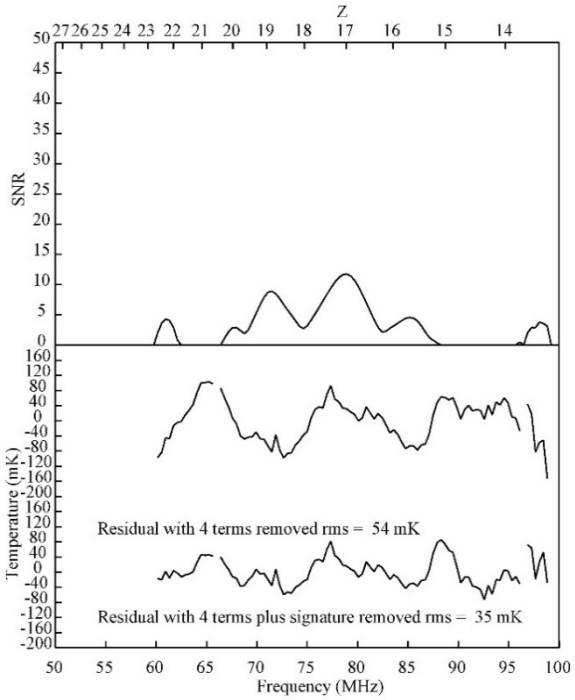

Figure 5

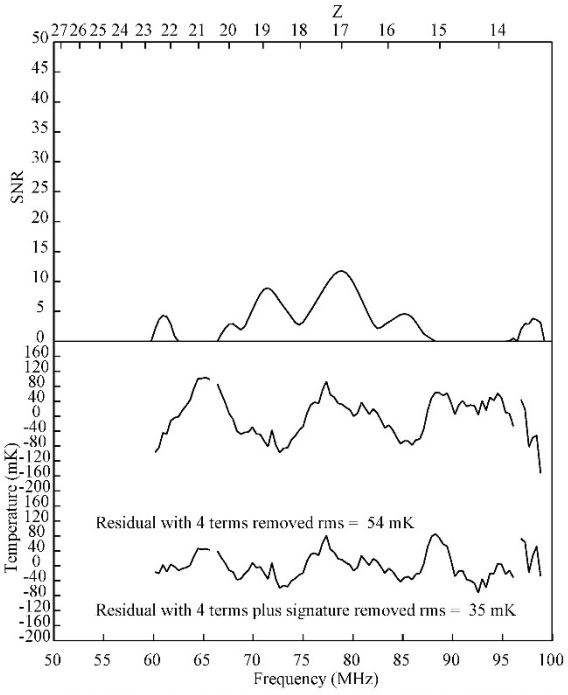

Figure 6

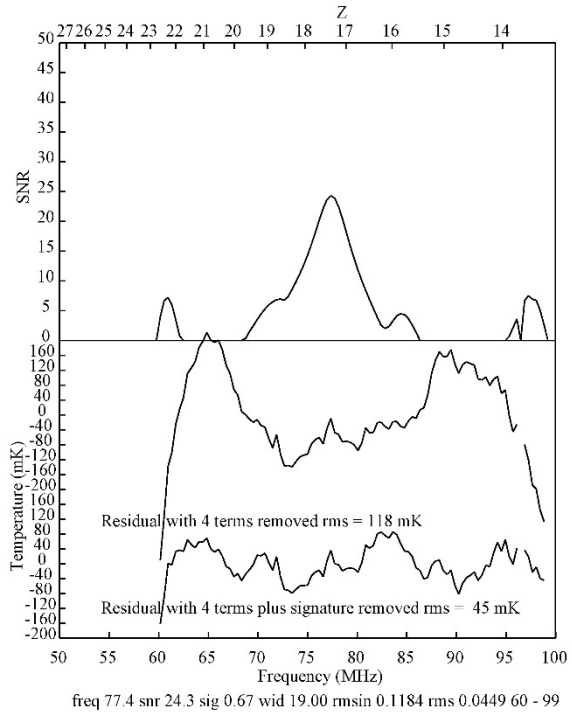

Figure 7.

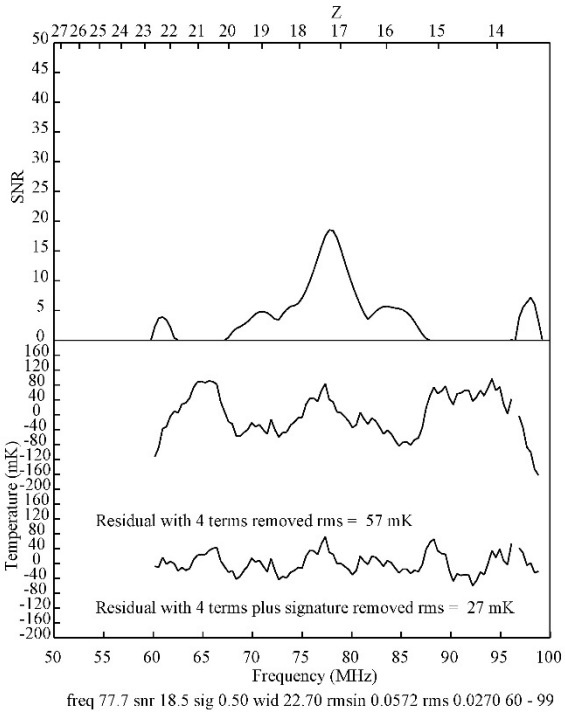

Figure 8.

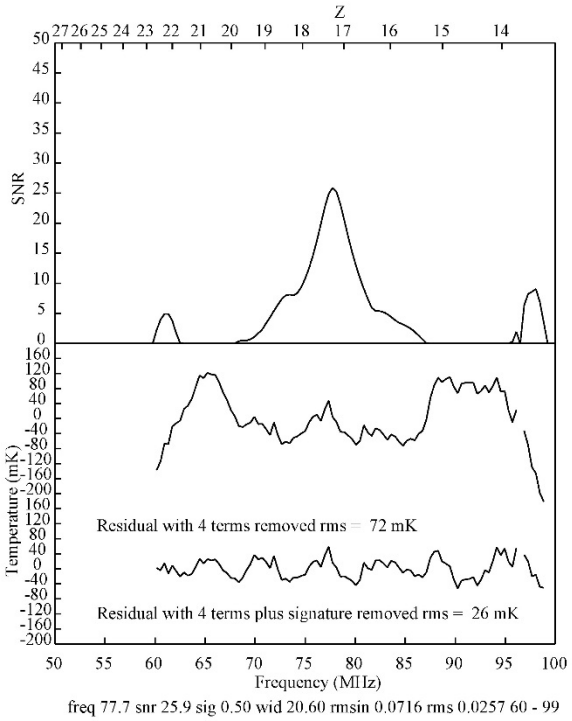

freq 77.7 snr 25.9 sig 0.50 wid 20.60 rmsin 0.0716 rms 0.0257 60 - 99

Figure 9.

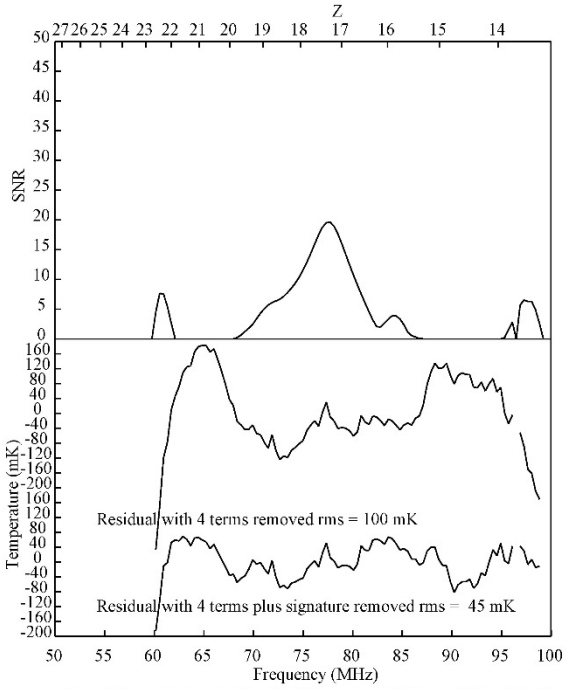

freq 77.7 snr 19.6 sig 0.62 wid 20.10 rmsin 0.0996 rms 0.0451 60 - 99

Figure 10.

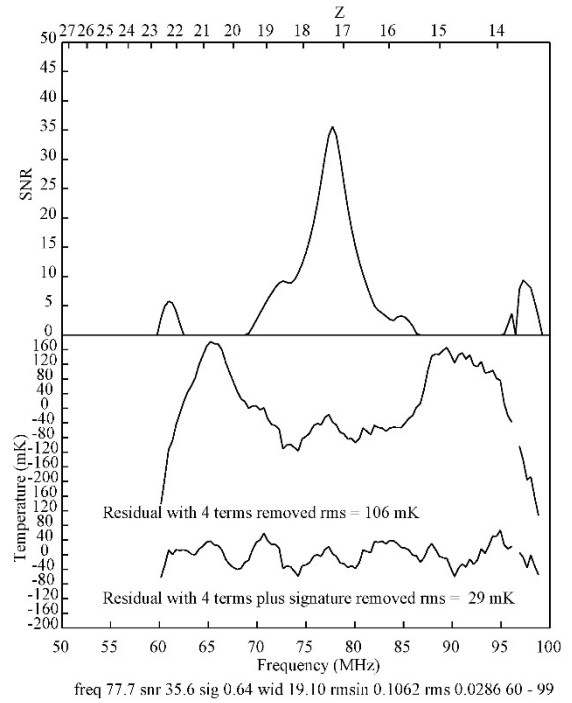

freq 77.7 snr 35.6 sig 0.64 wid 19.10 rmsin 0.1062 rms 0.0286 60 - 99

Figure 11.

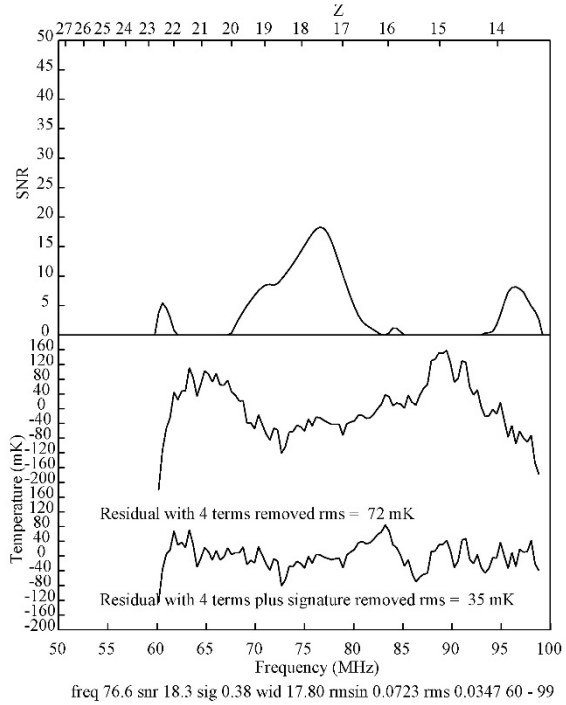

freq 76.6 snr 18.3 sig 0.38 wid 17.80 rmsin 0.0723 rms 0.0347 60 - 99

Figure 12.